Desalination and Water Treatment
www.deswater.com

doi: 10.5004/dwt.2017.20661

77 (2017) 69–74
May

Analysis of membrane fouling in a pilot-scale microfiltration plant using mathematical model and artificial neural network model

Younjong Park[a], Yongjun Choi[b], Sangho Lee[b,*]

[a]*Research Center, SK Engineerign & Construction, SK E&C Building, 192-18 Gwanhoon-dong, Jongno-gu, Seoul 100-130, Korea*
[b]*School of Civil and Environmental Engineering, Kookmin University, Jeongneung-Dong, Seongbuk-Gu, Seoul 136-702, Korea, Tel. +82-2-910-4529; Fax: +82-2-910-4939; email: sanghlee@kookmin.ac.kr*

Received 6 October 2016; Accepted 21 November 2016

ABSTRACT

Since membrane fouling is one of major challenges in hollow fiber microfiltration (MF) membrane processes, many studies have been done to analyze and control it in laboratory-scale systems. However, relatively few works have been accomplished for fundamental understanding of the fouling in pilot- or full-scale systems. Accordingly, this study intended to predict membrane fouling in a pilot-scale MF plant using a mathematical model and a statistical model based on artificial neural network (ANN). The effects of temperature, turbidity, total organic carbon, total operating time, and filtration time after chemical cleaning on the membrane fouling were considered. The major fouling mechanism was determined to be cake formation regardless of feed water quality changes. The cake formation model was found to be useful in explaining the membrane fouling in the short-term prediction of pilot-scale hollow fiber submerged membrane system. The results of application of the ANN model indicated high correlation coefficient between the measured and predicted output variables. Therefore, it appears that the ANN model is applicable in the long-term prediction of the membrane performance at different water qualities of the pilot-scale system.

Keywords: Microfiltration; Mathematical model; Artificial neural network; Drinking water; Submerged

1. Introduction

As the regulations for the drinking water quality have been increasingly stringent, the use of microfiltration (MF) membrane processes has rapidly grown in water treatment industry [1]. MF offers an effective method to remove particles and pathogenic microorganisms for drinking water production [2–4]. MF has advantages over other treatment techniques including high membrane surface area to footprint ratio, high mechanical strength, and backwashing capability at low module and energy cost compared with alternatives such as plate and frame, spiral wound, or tubular membranes [5–7]. However, a major obstacle to further incorporation of MF membrane processes in water treatment plants is flux reduction by contaminants or foulants in surface water [8]. Membrane fouling may result from bacteria, algae, inorganic colloids, and organic material depending on the quality of feed water [9]. Moreover, the prediction of membrane fouling is even challenging especially when the foulants in feed water vary with time [10,11].

Understanding the filtration behavior of hollow fibers is important to improve operation and design of the hollow fiber system. Although many studies have been done, they were mostly carried out using laboratory-scale equipments, which may not match with fouling behaviors in pilot- or full-scale systems. Accordingly, this study focused on the investigation of the fouling characteristics of a pilot-scale submerged hollow fiber MF membrane system. Using both mathematical and statistical models, long-term operation data from the pilot plant were analyzed. The effects of temperature, turbidity, total organic carbon (TOC), total operating time, and filtration time after chemical cleaning on the membrane fouling were considered.

* Corresponding author.

2. Theory

2.1. Mathematical model

MF membranes are designed to remove particulates from water via the sieving mechanism. Therefore, particle fouling resulting from the deposition of colloids and suspended solids on membranes remains a common phenomenon in MF systems. It is thus necessary to develop a model to predict and/or monitor membrane fouling for efficient operation of MF. In this study three membrane fouling models for constant flux system shown as Table 1 were applied to explain the transmembrane pressure (TMP) increase associated with particle deposition during membrane filtration: the pore blockage, pore constriction, and cake formation models [12–14]. Pore blocking and constriction are internal membrane fouling mechanisms, while cake formation occurs on the surface of membrane and is defined as external fouling [14]. The prediction of the fouling models was done based on the most widely used criteria, R^2. Once the minimum for R^2 was obtained, the R^2 values for three models were compared to determine the major fouling mechanism for the given pilot plant operating data.

2.2. Artificial neural network model

Although the mathematical models can be used to analyze fouling characteristics in hollow fiber membrane process, their application is limited to short-term operating data (order of hours and days). During long-term operation of MF systems, the feed water qualities such as turbidity, TOC and temperature, and membrane conditions change along operating time, which make it impossible to apply the mathematical model. Accordingly, it was necessary to use the artificial neural network (ANN) model to deal with the long-term pilot-scale operating data.

ANN model is an information processing system that is inspired by the way such as biological nervous systems, e.g., brain. The objective of a neural network is to compute output values from input values by some internal calculations [14]. In this study, ANN model was used to predict the membrane filtration performance with a multilayer perceptron (MLP) network that had a backpropagation training algorithm. The MLP consists of three or more layers of neurons called node: one input layer, one output layer, and one or more hidden layers. Each layer is fully connected to the next one. Fig. 1 shows a single node of a neural network. Inputs are represented by x_1, x_2, and x_i, and the output by y_j. There may be many input signals to a node. The node manipulates the inputs to give a single output signal. The strength of each connection, referred to its connection weight, may be adaptive coefficients within the network that determine the intensity of the input signal. Input data are presented to the network through the input layer, the values of which are denoted by x_i. Every input is multiplied by its corresponding weight, and the node uses summation of these weighted inputs ($W_{ij} \times x_1$) to estimate an output signal using a transfer function. These weighted inputs are then summed and added to a threshold value (θ_j) to produce the node input (I_j) as shown in the equation below:

$$I_j = \sum_{i=1}^{n} (W_{ij} \times x_i) + \theta_j$$

The node input (I_j) is then passed through an activation function, $f(I_j)$, to produce the node output, y_j. This node output is then used to compute the inputs for nodes in the following layer, until the final output is calculated [15]. Neural network predictions were quantitatively evaluated using the mean squared error (MSE):

$$\text{MSE} = \frac{\sum (P_i - O_j)^2}{n}$$

where P_i is the ith predicted value of the normalized resistance; O_i is the corresponding observed value; and n is the number of observation.

Table 1
Fouling models for MF

Fouling type	Equation	Constant parameter
Pore blocking model	$1-\left(\frac{P}{Po}\right)^{-1} = \alpha t$	α
Pore constriction model	$1-\left(\frac{P}{Po}\right)^{-\frac{1}{2}} = \beta t$	β
Cake formation model	$P - Po = \gamma t$	γ

Note: P – transmembrane pressure; P_0 – initial transmembrane pressure; t – operating time; α – pore blocking model parameter; β – pore constriction model parameter; and γ – cake formation model parameter.

3. Materials and methods

3.1. Feed water and membranes

The raw water collected from Han-river was used as the feed water after the coagulation pretreatment using

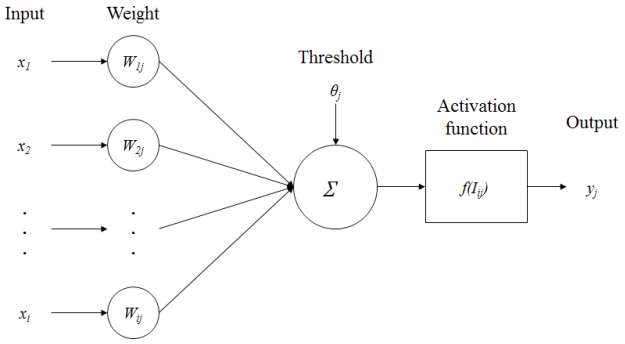

Fig. 1. Schematic diagram of a multilayer feed forward neural network.

polyaluminum chloride. A hollow fiber membrane (Lotte Chemical, Korea) made of polyvinylidene difluoride was used for all filtration experiments.

3.2. Pilot-scale membrane system

A pilot-scale submerged filtration system (1,000 m^3/d) shown as Fig. 2 was operated to examine the MF efficiency under various operating conditions. The system was automatically operated, and the data was collected using a computer. The results were analyzed in terms of the TMP. Operating conditions are as follows: 40-min filtration, and 1-min backwash with permeate and pressurized air.

4. Results and discussion

4.1. Raw water quality

Fig. 3 shows the variation in the quality of the feed water that was used for membrane filtration. The turbidity, TOC, and temperature in the raw water significantly changed with time. The turbidity, TOC, and temperature of the feed water were 1.5–81.5 NTU, 1.14–8.80 mg/L, and 2.0°C–29.0°C, respectively. In summer (from June to August), the feed water turbidity remained high due to frequent rains. The TOC was high in summer (from June to mid-August) and spring (from min-February to March). In addition to the feed water quality, the temperature also significantly affected the filtration efficiency. The average temperature of the water in winter was only 3.0°C, and in summer, 23.0°C. The low temperature in winter increased the viscosity by about 42% and thus reduced the pure water flux by 42%.

4.2. Model fit to the experimental data using the mathematical models

To investigate the fouling characteristics of the hollow fiber membrane in pilot-scale systems, the simple mathematical models (pore blockage, pore constriction, and cake formation model) were applied to the experimental data. The pilot-scale submerged filtration system was operated for a year. Fig. 4 shows the variations in the TMP in whole operating period. The TMP significantly depended on the raw water quality. The TMP remained low under 20 kPa

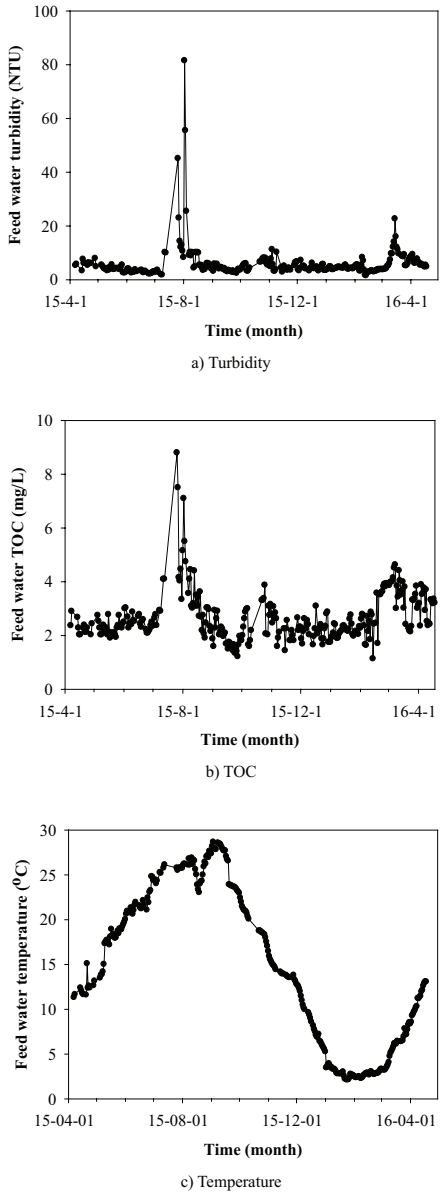

Fig. 3. Seasonal variations in the feed water quality: (a) turbidity, (b) TOC, and (c) temperature.

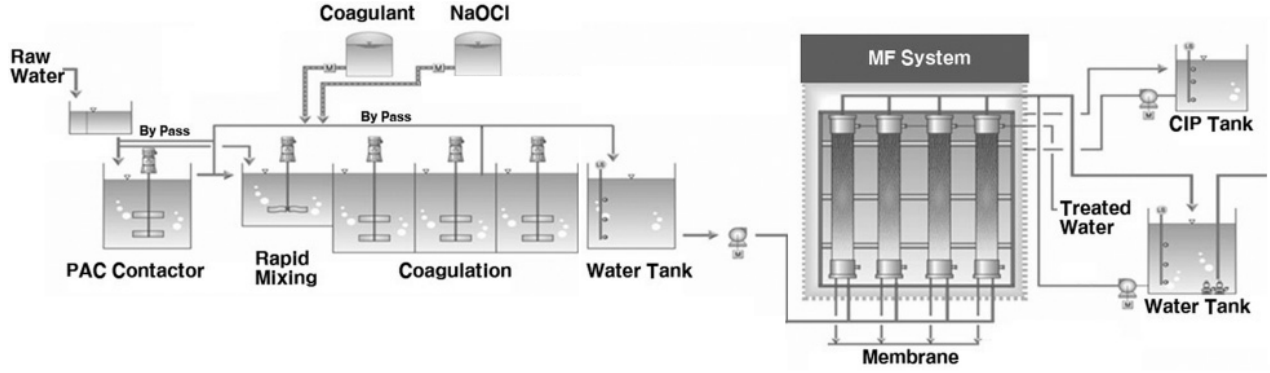

Fig. 2. Schematic diagram of the pilot plant.

from April to August although the TMP continuously increased due to membrane fouling because the turbidity and TOC of feed water remained low during this operating period. The TMP rapidly increased to a level about the August because of high turbidity and TOC. From October to February, the TMP dramatically increased because of the decreased water temperature. From mid-February to April, the TMP decreased in spite of high TOC because the feed water temperature greatly increased. Accordingly, the TMP was found to be sensitive to the seasonal variation in feed water quality. Therefore, it can be concluded that the TMP properly reflects the seasonal differences in the feed water quality.

The TMP corrected at 20°C was applied for model fits to exclude effect of the changes in feed water temperature. The operating period was separated into six parts in accordance with clean in place. To find the dominant membrane-fouling mechanism, the R^2 was analyzed, and the model evaluation criteria were selected. The results of model fits using different mathematical models are summarized in Table 2. As shown in Table 2 and Fig. 5, the cake formation model showed the highest level of agreement among the three models in all cases. The model parameter of cake formation model, γ, was calculated from 0.03 to 0.33 kPa/d, and R^2 was determined from 0.74 to 0.94. In the winter season (parts 4 and 5) the value of γ was the highest even though the effect of the changes in feed water temperature was excluded because the efficiency of physical and chemical cleaning decreased. In the summer season (part 2), the value of γ was also high because of high turbidity and TOC due to the frequent rains. In the autumn season (part 3) the value of γ was the lowest because of low turbidity and TOC. In the spring season (part 1) the value of γ was similar to that of part 5 because of high TOC. Accordingly, the fouling rate was found to be sensitive to the seasonal variation in feed water quality.

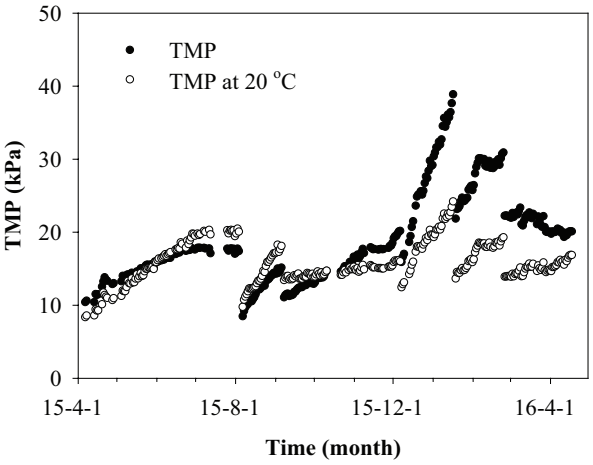

Fig. 4. Changes in the TMP in the pilot-scale MF system.

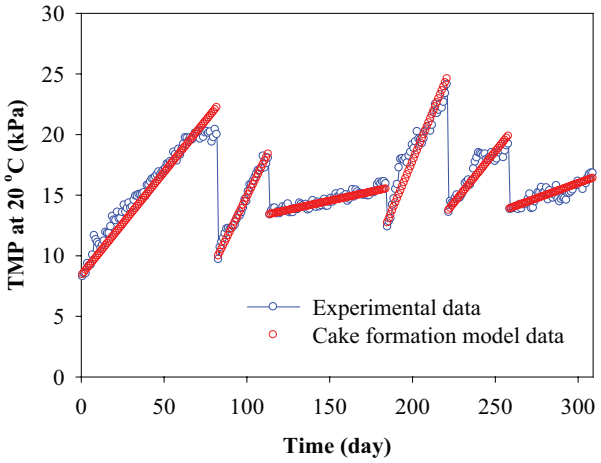

Fig. 5. Comparison of the model fit of cake formation model with the experimental data.

Table 3
The properties of the ANN model

Network inputs	Total operating time, filtration time after CIP, turbidity, TOC, temperature
Network outputs	TMP
Network type	Feed forward back propagation
Training function	Levenberg–Marquardt
Performance function	Mean squared error
Number of hidden layers	1
Number of neurons in hidden layer	10

Table 2
Comparison of a model parameter for each filtration model

Part	Pore blocking model		Pore constriction model		Cake formation model	
	A (1/d)	R^2	β (1/d)	R^2	γ (kPa/d)	R^2
1 (April to July)	0.68	0.22	0.56	0.64	0.17	0.93
2 (August to min-September)	1.75	0.82	0.99	0.89	0.28	0.96
3 (min-September to mid-November	0.22	0.81	0.11	0.82	0.03	0.85
4 (mid-November to mid-January)	1.57	0.52	0.88	0.63	0.33	0.86
5 (mid-January to February)	0.94	0.73	0.51	0.75	0.18	0.81
6 (March to April)	0.29	0.72	0.15	0.71	0.05	0.74

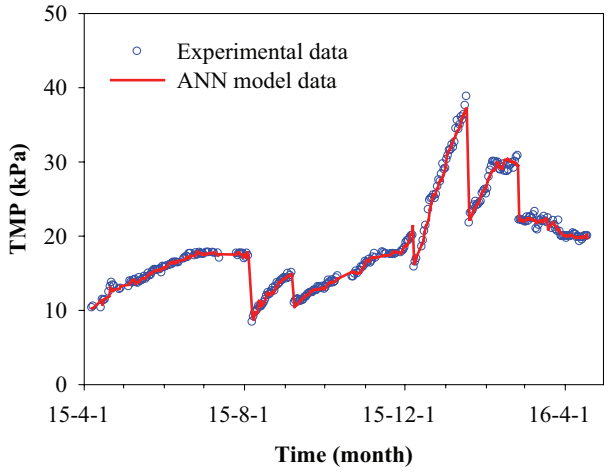

Fig. 6. Comparison of the model fit of ANN model with the experimental data.

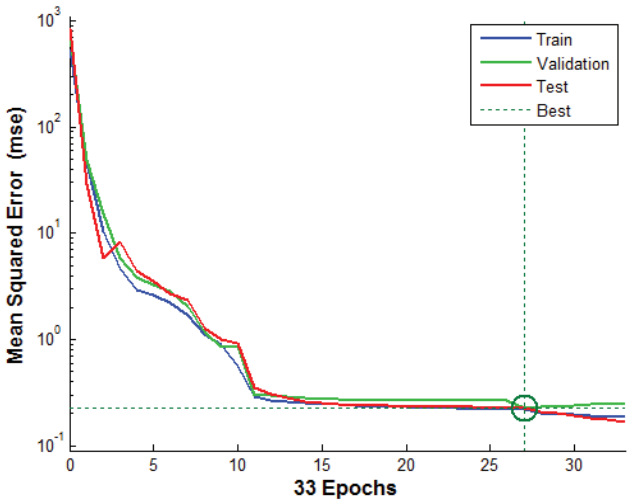

Fig. 7. MSE as a function of the number of iterations.

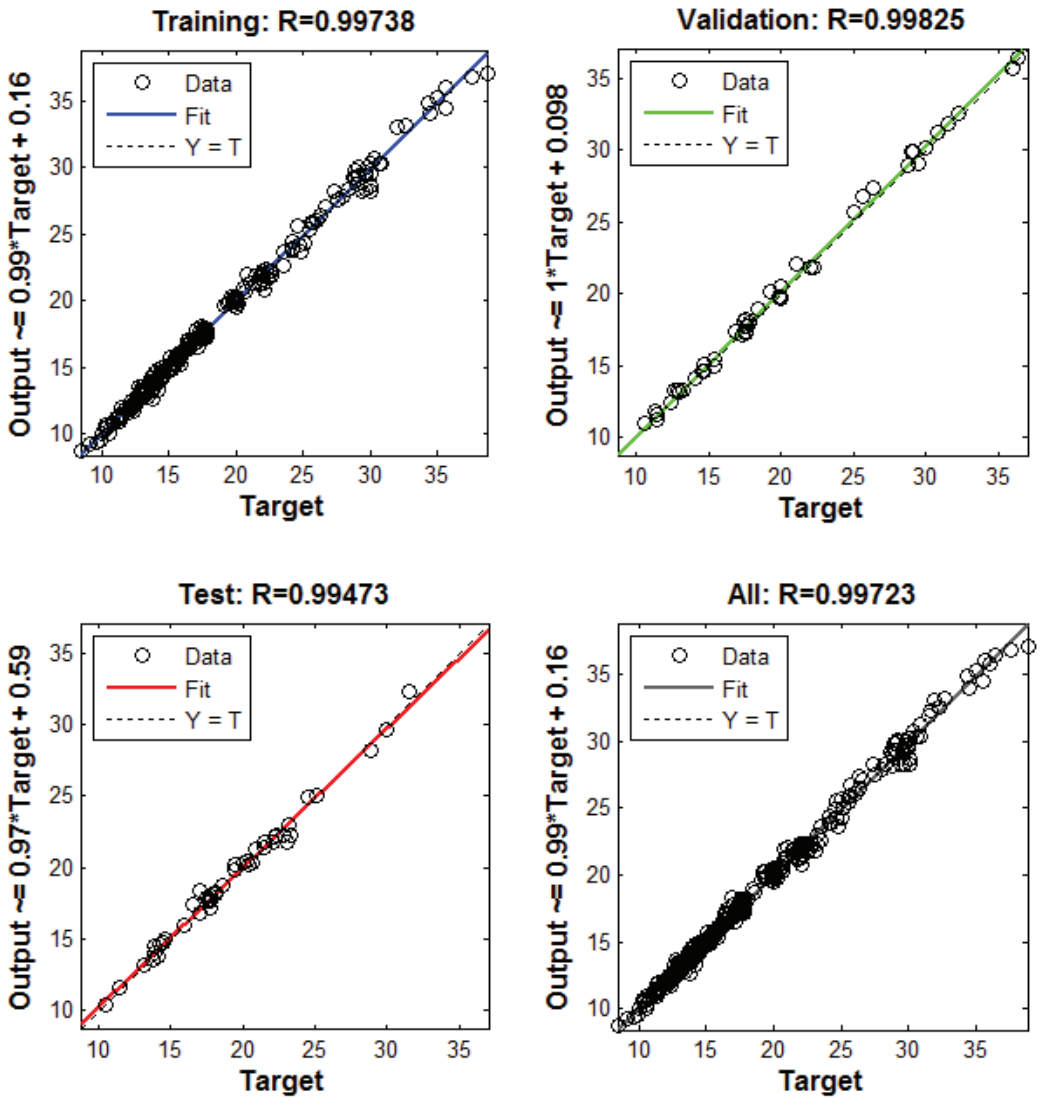

Fig. 8. ANN model regression of training, test, validation, and all data.

4.3. Model fit to the experimental data using the ANN model

ANN model was developed to simulate the performance of the pilot-scale submerged membrane system. In this study, the ANN model was created in MATLAB software that offers a platform for the simulation application. MATLAB toolbox opens the network/data manager window, which allows the user to import, create, use, and export neural networks and data. The properties of the ANN model are presented in Table 3.

The operating data and feed water qualities were collected over 1-year period. This period was satisfactory as it covers all probable seasonal variations in the studied variables. The application randomly divides input vectors and target vectors into three sets as follows: 70% are used for training; 15% are used to validate that the network is generalizing and to stop training before over-fitting; and the last 15% are used as a completely independent test of network generalization. Fig. 6 shows the experimental and predicted values of the TMP as a function of the operating time. The predicted values from the model matched the experimental values very well. The performances of the ANN model were evaluated using the correlation coefficient (R) and MSE.

Fig. 7 shows the MSE and the number of iterations. A sharp drop in the MSE in the first a few iterations (fast training) is shown. The training cycles stopped after 33 iterations, with a smallest MSE value of 0.226 at 27 iterations.

The ANN models showed high strength and a linear relationship direction between the predicted data and experimental data. It is observed that the output tracks the targets very well for training (R value = 0.99973), validation (R value = 0.9982), and testing (R value = 0.9947) as shown in Fig. 7. These values can be equivalent to a total response of R value = 0.9972. This suggests that the ANN model has the potential for long-term (order of month) prediction of the membrane performance in pilot-scale systems in the presence of seasonal variations of raw water quality.

5. Conclusion

In this study, the fouling characteristics of pilot-scale hollow fiber submerged MF system were investigated using the simple mathematical fouling models and the ANN model. The following conclusions were drawn:

- The seasonal variations in the feed water quality significantly affected the fouling characteristics of Korean river water.
- Among three fouling models, the cake formation model was found to be the most suitable to explain the membrane fouling in the short-term (order of hours and days) prediction of pilot-scale MF system.
- The ANN model was successfully applied to interpret the long-term operation data of the MF system. The high correlation coefficient (R value) between the measured and predicted output variables was up to 0.99. This result suggests that the ANN model is capable of predicting long-term behaviors of pilot MF systems even under seasonal variations of raw water qualities.

Acknowledgment

This research was supported by a grant (12-TI-C01) from Advanced Water Management Research Program funded by Ministry of Land, Infrastructure and Transport of Korean government and was also supported by Korea Ministry of Environment as The Eco-Innovation project (Global Top project, Project no. GT-SWS-15-01-002-0).

References

[1] American Water Works Association, Microfiltration and Ultrafiltration Membranes for Drinking Water, Denver, 2008.
[2] S.S. Adham, J.G. Jacangelo, J.M. Laine, Characteristics and costs of MF and UF plants, J. Am. Water Works Assn., 88 (1996) 22–31.
[3] J.G. Jacangelo, N.L. Patania, J.M. Lain, J.M. Montgomery, W. Booe, J. Mallevialle, Low Pressure Membrane Filtration for Particle Removal, AWWA Research Foundation, Denver, 1992.
[4] J.G. Jacangelo, S.S. Adham, J.M. Laine, Mechanism of Cryptosporidium, Giardia, and MS2 Virus Removal by MF and UF, J. Am. Water Works Assn., 87 (1995) 107–121.
[5] A.G. Fane, S. Chang, E. Chardon, Submerged hollow fibre membrane module design options and operational considerations, Desalination, 146 (2002) 231–236.
[6] P. Aptel, C.A. Buckley, Categories of Membrane Operations, J. Mallevialle, P.E. Odenaal, M.R. Wiesner, Eds., Water Treatment Membrane Processes, McGraw Hill, New York, 1996.
[7] L.J. Zeeman, A.L. Zydney, Microfiltration and Ultrafiltration: Principles and Applications, Marcel Dekker, New York, 1996.
[8] B. Nicolaisen, Developments in membrane technology for water treatment, Desalination, 153 (2003) 355–360.
[9] S. Chellam, J. Jacangelo, T. Bonacquisti, Modelling and experimental verification of pilot-scale hollow, direct flow microfiltration with periodic backwashing, Environ. Sci. Technol., 32 (1998) 75–81.
[10] B. Tenzer, A. Adin, M. Priel, Seawater filtration for fouling prevention under stormy conditions, Desalination, 125 (1999) 77–88.
[11] S. Babel, S. Takizawa, H. Ozaki, Factors affecting seasonal variation of membrane filtration resistance caused by Chlorella algae, Water Res., 36 (2002) 1193–1202.
[12] A.S. Ward, Liquid Filtration Theory, M.J. Matteson, C. Orr, Eds., Filtration, Principles and Practices, Marcel Dekker, New York, 1987, pp. 131–161.
[13] J. Granger, J. Dodds, D. Leclerc, Filtration of low concentrations of latex particles on membrane filters, Filtr. Sep. (January/February) (1985) 58–60.
[14] V.N. Delgrange, N. Cabassud, M. Cabassud, L. Durand-Bourlier, J.M. Laine, Neural networks for prediction of ultrafiltration transmembrane pressure: application to drinking water production, J. Membr. Sci., 150 (1998) 111–123.
[15] Q.F. Liu, S.H. Kim, Evaluation of membrane fouling models based on bench-scale experiments: a comparison between constant flowrate blocking laws and artificial neural network (ANNs) model, J. Membr. Sci., 310 (2008) 393–401.